Silencing the conserved small nuclear ribonucleoprotein SmD1 target gene alters susceptibility to root-knot nematodes in plants

Joffrey Mejias, Yongpan Chen, Jérémie Bazin, Nhat-My Truong, Karine Mulet, Yara Noureddine, Stéphanie Jaubert-Possamai, Sarah Ranty-Roby, Salomé Soulé, Pierre Abad, et al.

▶ **To cite this version:**

Joffrey Mejias, Yongpan Chen, Jérémie Bazin, Nhat-My Truong, Karine Mulet, et al.. Silencing the conserved small nuclear ribonucleoprotein SmD1 target gene alters susceptibility to root-knot nematodes in plants. Plant Physiology, 2022, 189 (3), pp.1741-1756. 10.1093/plphys/kiac155 . hal-03879983

HAL Id: hal-03879983
https://hal.science/hal-03879983v1

Submitted on 30 Nov 2022

HAL is a multi-disciplinary open access archive for the deposit and dissemination of scientific research documents, whether they are published or not. The documents may come from teaching and research institutions in France or abroad, or from public or private research centers.

L'archive ouverte pluridisciplinaire **HAL**, est destinée au dépôt et à la diffusion de documents scientifiques de niveau recherche, publiés ou non, émanant des établissements d'enseignement et de recherche français ou étrangers, des laboratoires publics ou privés.

RESEARCH ARTICLE

SHORT TITLE: *SmD1,* a susceptibility gene to nematodes

Authors for Contact : Bruno Favery and Michaël Quentin (Tel +33492386495; bruno.favery@inrae.fr and michael.quentin@inrae.fr).

TITLE: Silencing the conserved *SmD1* target gene alters susceptibility to root-knot nematodes in plants

Joffrey Mejias[1], Yongpan Chen[1], Jérémie Bazin[2], Nhat-My Truong[1], Karine Mulet[1], Yara Noureddine[1], Stéphanie Jaubert-Possamai[1], Sarah Ranty-Roby[1], Salomé Soulé[1], Pierre Abad[1], Martin D. Crespi[2], Bruno Favery[1,*] and Michaël Quentin[1,*]

[1] INRAE, Université Côte d'Azur, CNRS, ISA, F-06903 Sophia Antipolis, France

[2] Institute of Plant Sciences Paris-Saclay (IPS2), CNRS, INRA, Universités Paris Saclay, Evry, Université de Paris, 91192 Gif sur Yvette, France

ONE SENTENCE SUMMARY: The conserved spliceosomal SmD1 protein targeted by EFF18s effectors is involved in plant susceptibility to root-knot nematodes

List of author contributions : J.M. designed and performed experiments, and interpreted data; J.M., Y.C. and N.M.T. generated constructs and performed yeast two-hybrid analysis; Y.C. and

S.R.R. performed *in situ* hybridisations. Y.C. performed *in planta* subcellular localisation experiments; K.M. performed VIGS and nematode infection tests in tomato; S.S. analyzed RT-qPCR data. J.B., YN, S.J.P. and M.D.C. performed the tomato transcriptome analysis and analyzed AS data; J.M., JB., S.J.P., P.A., M.D.C., B.F. and M.Q. wrote the manuscript; B.F. and M.Q. obtained funding, designed the work and supervised the experiments and data analyses; all the authors read and edited the manuscript.

Funding information: This work was funded by the INRAE SPE department, by the French Government (National Research Agency, ANR) through the LabEx Signalife (#ANR-11-LABX-0028-01), the LabEx Saclay Plant Sciences (#ANR-10-LABX-40) and the project MASH (#ANR-21-CE20-0002), by the INRAE-Syngenta Targetome project, by the French-Japanese bilateral collaboration programmes PHC SAKURA 2016 #35891VD and 2019 #43006VJ and by the French-Chinese bilateral collaboration program PHC XU GUANGQI 2020 #45478PF. J.M. held a doctoral fellowship from the French *Ministère de l'Enseignement Supérieur, de la Recherche et de l'Innovation* (MENRT grant). N.M.T. was supported by a USTH fellowship, as part of the 911-USTH programme of the Ministry of Education and Training of The Socialist Republic of Vietnam. Y.C. obtained scholarships from the China Scholarship Council (No. 201806350108) for studies at INRAE, France.

Present addresses: J.M. Department of Plant Pathology and Microbiology, Iowa State University, Ames, IA 50011, U.S.A.; Y.C. Department of Plant Pathology and Key Laboratory of Pest Monitoring and Green Management of the Ministry of Agriculture, China Agricultural University, 100193 Beijing, China; N.M.T. Vietnamese - German Center for Medical Research (VG-CARE),

Hanoi, Vietnam

*Authors for Contact : Bruno Favery and Michaël Quentin (bruno.favery@inrae.fr and michael.quentin@inrae.fr).

Word count: 6979 words (Introduction, 952; Results, 2035; Discussion, 1887; Experimental procedures, 2105; Acknowledgements, 243). **Figures:** 7. **Supplementary informations:** 16 (8 tables, 9 figures).

Abstract

Root-knot nematodes (RKNs) are among the most damaging pests of agricultural crops. Indeed, *Meloidogyne* is an extremely polyphagous genus of nematodes that can infect thousands of plant species. A few genes for resistance (R-genes) to RKN suitable for use in crop breeding have been identified, and new virulent strains and species of RKN have emerged rendering these R-genes ineffective. Secretion of RKN effectors targeting plant functions, mediate the reprogramming of root cells into specialised feeding cells, the giant cells, essential for RKN development and reproduction. Conserved targets among plant species define the more relevant strategies for controlling nematode infection. The EFFECTOR 18 protein (EFF18) from *M. incognita* interacts with the spliceosomal protein SmD1 in Arabidopsis, disrupting its function in alternative splicing regulation and modulating the giant cell transcriptome. We show here that EFF18 is a conserved RKN-specific effector that targets this conserved spliceosomal SmD1 protein in Solanaceae. This interaction modulates alternative splicing events produced by *Solanum lycopersicum* in response to *M. incognita* infection. The alteration of *SmD1* expression by virus-induced gene silencing

(VIGS) in Solanaceae affects giant cell formation and nematode development. Thus, our work defines a new promising conserved *SmD1* target gene to develop broad resistance for the control of *Meloidogyne* spp. in plants.

Introduction

Plant parasitic nematodes are major crop pests causing crop losses of several billion dollars annually, through damage to almost all cultivated plants (Singh *et al.*, 2013). Root-knot nematodes (RKNs) of the genus *Meloidogyne* are considered to be the most detrimental of these plant parasites, due to the magnitude of the economic losses they cause (Jones *et al.*, 2013). RKNs are widespread worldwide and can infect more than 5,500 different plant species, including many species of major agricultural interest. About 100 RKN species have been described, and those reproducing asexually by mitotic parthenogenesis (*M. incognita*, *M. javanica*, *M. arenaria* and *M. enterolobii*) are the most polyphagous and damaging pests. By contrast, those reproducing sexually or by meiotic parthenogenesis (*M. hapla*) have a smaller host range (Blok *et al.*, 2008; Castagnone-Sereno, 2006).

All RKNs are sedentary endoparasites that induce the formation of specialised feeding structures and typical root deformations, known as galls or root knots, that deprive the plant of nutrients (Escobar *et al.*, 2015; Favery *et al.*, 2016). After hatching from eggs, the stage 2 juveniles (J2) of *M. incognita* penetrate the root apex and migrate between plant cells to reach the plant vascular system (Holbein *et al.*, 2019). Once there, the filiform J2 switch to a sedentary lifestyle, by selecting five to seven cells of the vascular parenchyma and inducing their reprogramming into specialised feeding cells, known as giant cells (Escobar *et al.*, 2015; Favery *et al.*, 2016; Olmo *et al.*, 2020). These giant cells act as metabolic sinks close to the xylem and phloem vessels that withdraw water and nutrients from the sap (Rodiuc *et al.*, 2014). The nematode uses these specific giant cells for feeding for the rest of its life. After successive moults, the sedentary swollen juveniles develop into an adult female that lays her egg masses on the root surface, thus completing the cycle. The giant cells are hypertrophied and multinucleate, harbouring hundreds of

nuclei. They are produced by successive nuclear divisions uncoupled from cytokinesis, followed by nuclear endoreduplication (de Almeida Engler and Gheysen, 2013). RKN induce giant cells and gall formation by recruiting the developmental pathways of post-embryonic organogenesis and regeneration to promote transient pluripotency (Olmo *et al.*, 2020).

RKNs parasitise plants and induce the redifferentiation of vascular cells into giant cells by secreting effectors, molecules that recruit/hijack plant functions (Mejias *et al.*, 2019; Toruño *et al.*, 2016). RKN effectors, particularly those produced by the three oesophageal gland cells and secreted into the host through a stylet, are involved in the four main functions underlying parasitism: (i) the degradation and modification of plant cell walls during J2 migration within the root; (ii) the suppression of host defences; (iii) the reprogramming of plant vascular cells as giant cells and (vi) the maintenance of these feeding sites (Mitchum *et al.*, 2013; Truong *et al.*, 2015). The profound morphological and metabolic changes associated with giant cell induction by RKNs and the transcriptional reprogramming occurring during the formation of these cells require the secretion of effectors targeting key nuclear functions (Hewezi and Baum, 2013; Quentin *et al.*, 2013). With the exception of plant cell wall-degrading enzymes (Danchin *et al.*, 2010), very few effectors have been shown to be conserved and functional in multiple RKN species. For example, 16D10 encodes a conserved secretory peptide conserved in five RKN species (*M. incognita*, *M. arenaria*, *M. hapla*, *M. javanica*, *M. chitwoodi*) that stimulates root growth and functions as a ligand for a putative plant transcription factor (Huang *et al.*, 2006; Dinh *et al.*, 2015). The silencing of *16D10* by RNA interference methods confers broad resistance to RKNs (Huang *et al.*, 2006; Dinh *et al.*, 2015). The chorismate mutates, MiCM3 (Wang *et al.*, 2018) and MjCM1 (Doyle and Lambert, 2003), and the transthyretin-like proteins, MjTTL5 (Lin *et al.*, 2016) and MhTTL2 (Gleason *et al.*, 2017), also appear to be effectors conserved among RKNs. Interestingly, MhTTL2

120 is expressed in the amphids (Gleason *et al.*, 2017), whereas MjTTL5 is expressed specifically in
121 the subventral glands, suggesting different roles for these two molecules in parasitism, encoded by
122 the same gene family (Lin *et al.*, 2016).

123 The majority of plant protein-coding genes contain introns which are removed from precursor
124 messenger RNAs (pre-mRNA) to produce mRNAs during splicing. Alternative splicing (AS)
125 occurs when this process is regulated, producing more than one mRNA from the pre-mRNA and
126 giving rise to functionally different proteins (Reddy *et al.,* 2013; Staiger and Brown, 2013). AS
127 plays a crucial role in plant responses to biotic stress (Rigo *et al.,* 2019). Recent findings indicate
128 that pathogen effectors can modulate AS to corrupt host plant physiology and allow disease
129 development (Verma *et al.,* 2018; Huang *et al,.* 2020). In a previous study, we showed that
130 MiEFF18, a nuclear effector from *M. incognita,* is secreted *in planta*, targets the giant cell nuclei
131 and interacts with the SmD1 protein, a core component of the spliceosome (Mejias *et al.*, 2021).
132 We show here that MiEFF18 is a specific and conserved nuclear RKN effector and that
133 orthologous genes are specifically expressed in the salivary glands of RKNs. We also show that
134 MiEFF18 and its orthologue in *M. enterolobii,* MeEFF18, interact with SmD1 proteins from
135 different plant species to reprogram AS in the feeding site induced by *M. incognita* in tomato roots.
136 Interestingly, virus-induced gene silencing (VIGS) approaches to silence the *SmD1* genes of
137 *Nicotiana benthamiana* and *S. lycopersicum* greatly impaired RKN infection. These results are
138 consistent with the targeting, by RKNs, of conserved spliceosomal functions, to drive the
139 development of giant cells, facilitating parasitism on a large spectrum of host plants. This allowed
140 us to propose that the conserved interaction of EFF18 effectors and SmD1 can be the basis for a
141 new general strategy to control nematode infection in plants.
142

143

Results

EFF18 is a conserved RKN-specific effector targeting the plant nucleus

MiEFF18 was first described in the *M. incognita* genome (Mejias *et al.*, 2021; Nguyen *et al.*, 2018; Rutter *et al.*, 2014). Database queries showed that MiEFF18 displayed no sequence homology or known domains, and that it was absent from nematodes of other genera, such as cyst nematodes and free-living nematodes. By contrast, EFF18 orthologues were identified in seven of the eight RKNs for which genome sequences were available: *M. incognita*, *M. javanica*, *M. arenaria* (Blanc-Mathieu *et al.*, 2017), *M. hapla* (Opperman *et al.*, 2008), *M. enterolobii* (syn. *M. mayaguensis*) (Koutsovoulos *et al.*, 2020), *M. floridensis* (Lunt *et al.*, 2014) and *M. luci* (Susič *et al.*, 2020) (Figure 1, Supplemental Table S1, Supplemental Figure S1 and S2). No EFF18 orthologue was identified in *M. graminicola* (Somvanshi *et al.*, 2018). Three paralogous copies were identified, in the *M. incognita*, *M. javanica* and in *M. luci* genomes. Four copies were detected in *M. arenaria* and a single copy was detected in *M. hapla, M. floridensis* and *M. enterolobii*. A sequence alignment and analysis of the RKN EFF18 protein sequences showed that they were more than 60% identical, between 279 and 316 amino acids (aa) long and that they had an N-terminal secretion signal peptide (SP), a low-complexity acidic D/E-rich region and a C-terminal lysine (K)-rich region of unknown function carrying direct repeats (Figure 1A, Supplemental Figure S2). Only the C-terminal K-rich part displayed marked differences between copies.

A phylogenetic tree based on an alignment of the 17 RKN EFF18 protein sequences showed divergences between copies among the same species (Figure 1A). EFF18 proteins more closely related to MiEFF18a/Minc18636 harboured one monopartite NLS and one bipartite NLS, whereas other copies are more divergent (*e.g.* MiEFF18b/Minc15401 and MiEFF18c) and contained only

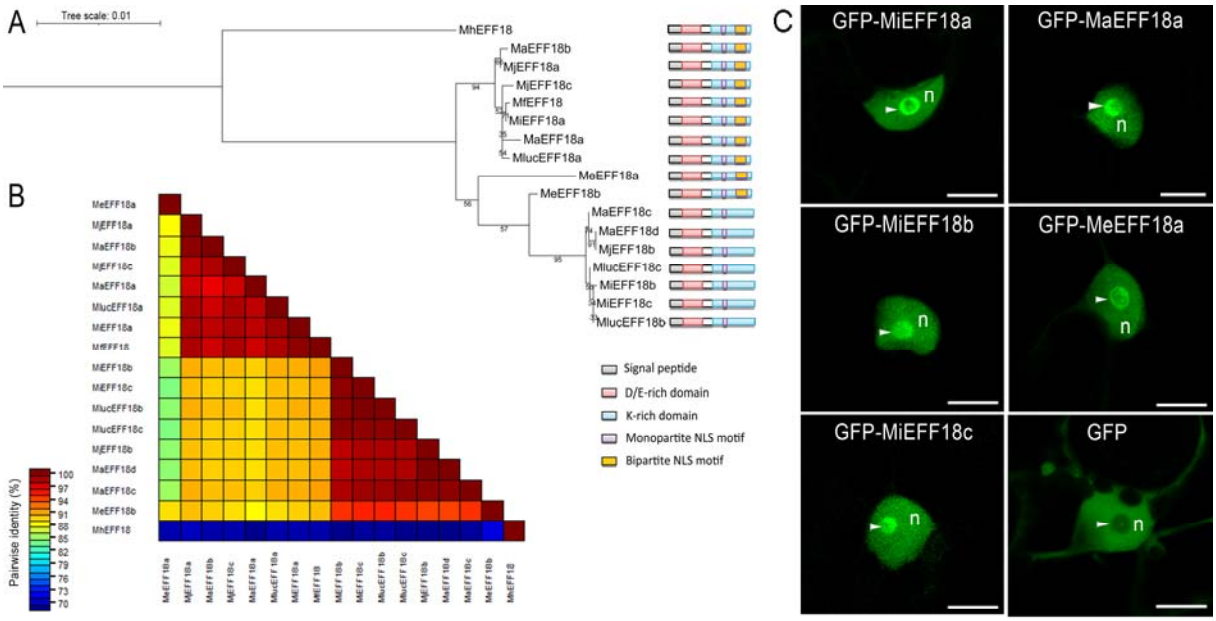

Figure 1 Effector 18 (EFF18) is a conserved effector in root-knot nematodes. A, Phylogenetic tree and schematic diagram of root-knot nematode EFF18 protein sequences. The tree scale corresponds to the number of substitutions per site based on the amino-acid matrix (JTT). In the schematic diagram of EFF18 proteins, the predicted secretion signal peptide (SP; grey boxes), the aspartic acid and glutamic acid (D-E)-rich region (red boxes), the lysine (K)–rich C-terminal region (blue boxes) and the nuclear mono- (purple boxes) or bi- (orange boxes) partite localisation signals (NLS) are shown. EFF18 proteins from the closest group to MiEFF18a carry one mono- and one bipartite NLS, whereas the most divergent copies have only a single monopartite NLS. B, Pairwise sequence identity matrix for RKN EFF18 protein sequences. C, EFF18 localised to the nucleus and nucleolus of plant cells. The MiEFF18s, MaEFF18a and MeEFF18a sequences were fused to that encoding GFP in a C-terminal position and expressed in *N. benthamiana* leaves by agroinfiltration. GFP was used as a control and gave fluorescence in the cytoplasm and the nucleus (n), but not the nucleolus (arrowhead). Bars = 10 µm.

one monopartite NLS (Figure 1A). The EFF18s with bipartite NLS were 98% to 100% identical to the MiEFF18a protein, whereas those with only monopartite NLS were only 79 to 89% identical to this protein (Figure 1B). *M. hapla* had the most divergent genome of the *Meloidogyne* species tested. It was found to have a single copy of the gene, 63-65% identical to the closest copies and the most divergent copies, which suggests that the ancestor of RKN species had an *EFF18* gene. *MiEFF18a*, *MiEFF18b*, *MiEFF18c*, *MaEFF18a* and *MeEFF18a* fused at their N-terminus to GFP were transiently expressed in *N. benthamiana* leaf epidermis. For all EFF18 constructs, including

174 *MiEFF18b* and *MiEFF18c* carrying a single monopartite NLS, GFP fluorescence was only
175 detected in the nucleus, with a strong GFP signal accumulating in the nucleolus (Figure 1C). In
176 contrast, GFP alone was detected in the cytoplasm and the nucleus, but not in the nucleolus (Figure
177 1C). Altogether, these results provide support for the role of EFF18 as a conserved nuclear
178 effector.
179
180 **RKN EFF18s are specifically expressed in the subventral glands**
181 MiEFF18 have been shown to be more strongly expressed at parasitic stages and to be expressed
182 specifically in the subventral glands of *M. incognita* J2s (Rutter *et al.*, 2014; Nguyen *et al.*, 2018;
183 Mejias *et al.*, 2020). We studied the pattern of expression of genes encoding orthologous
184 sequences of MiEFF18 in two other RKN species, by performing *in situ* hybridisation (ISH) for the
185 *M. enterolobii MeEFF18a* and the *M. arenaria MaEFF18a* sequences. A specific signal was
186 detected in the subventral oesophageal gland cells of pre-J2s after hybridisation with
187 digoxigenin-labelled *MeEFF18a* and *MaEFF18a* antisense probes (Figure 2). No signal was
188 detected in pre-J2s with sense negative controls. This finding suggests that MaEFF18a and
189 MeEFF18a, may, like MiEFF18a, be secreted and play an important role in nematode parasitism.
190
191 **MiEFF18a and MeEFF18a interact with the SmD1 proteins of *A. thaliana*, *N. benthamiana***
192 **and *S. lycopersicum***
193 We have demonstrated an interaction between MiEFF18a and the nuclear ribonucleoproteins
194 SmD1s from *S. lycopersicum* and *A. thaliana,* modulating the pattern of AS in *A. thaliana* and
195 promoting the formation of giant cells (Mejias *et al.*, 2021). Two genes, *AtSmD1a* (*AT3G07590*)
196 and *AtSmD1b* (*AT4G02840*), encode SmD1 proteins in *A. thaliana* (Koncz *et al.*, 2012). Most of

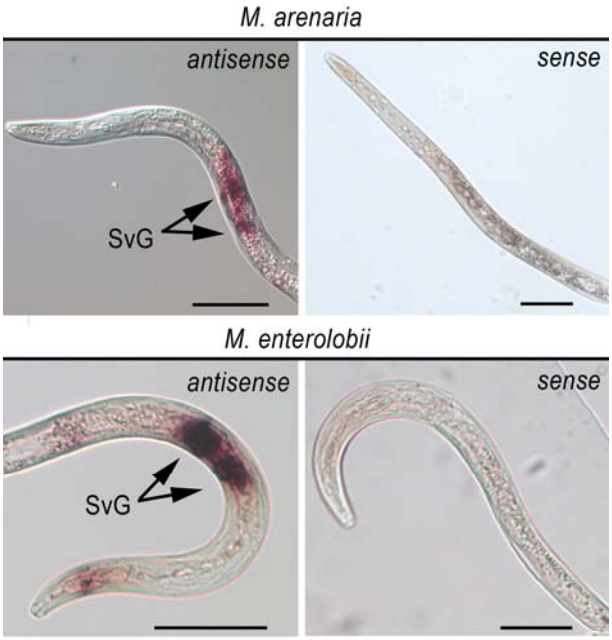

Figure 2 RKN EFF18s are specifically expressed in the subventral glands. *In situ* hybridisation, showing EFF18 transcripts in the subventral glands of J2s of *M. arenaria* and *M. enterolobii*. Sense probes for the *MaEFF18* and *MeEFF18* transcripts were used as a negative control. SvG, subventral glands. Bars = 40 µm.

the *Arabidopsis* SmD1 protein production is allowed by the expression of *AtSmD1b*, and the analysis of *smd1a* and *smd1b* knockout lines indicated that mostly *AtSmD1b* contributes to Arabidopsis development and susceptibility to nematodes (Elvira-Matelot *et al.*, 2016; Mejias *et al.*, 2021). According to RNAseq data, no difference in *AtSmD1a* and *AtSmD1b* expression was observed in galls 5 or 7 days following inoculation with *M. incognita*, when compared to uninfected roots (Mejias *et al.*, 2021). Two genes, sharing 98.0% nucleotide sequence identity, encode 100% identical proteins (SlSmD1) in *S. lycopersicum: SlSmD1a* (*Solyc06g084310*) and *SlSmD1b* (*Solyc09g064660*). In *N. benthamiana*, we identified three genes, sharing 89.0 to 97.1% nucleotide sequence identity, encoding SmD1s: *NbSmD1a* (*Niben101Scf01782g05006*), *NbSmD1b* (*Niben101Scf05290g01011*), and *NbSmD1c* (*Niben101Scf04283g03011*). *NbSmD1a*

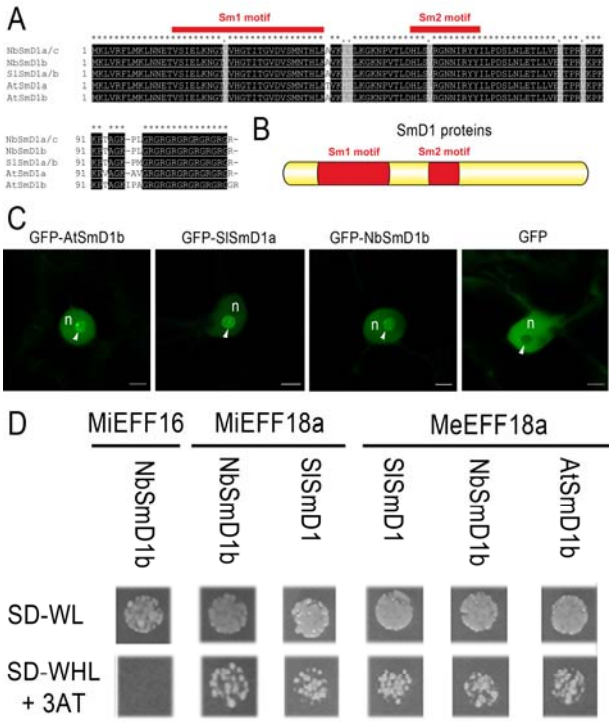

Figure 3 Conserved SmD1 proteins are targeted by EFF18. A, MAFFT protein sequence alignment of the *S. lycopersicum* (Sl), *N. benthamiana* (Nb) and *A. thaliana* (At) SmD1 proteins. B, Schematic representation of Sm1 and Sm2 motif in SmD1 proteins. C, GFP-AtSmD1b, GFP-SlSmD1a and GFP-NbSmD1b accumulate in the nucleus and particularly in the nucleolus when transiently expressed in *N. benthamiana* epidermal leaf cells. GFP was used as a nucleocytoplasmic control. n= nucleoplasm; White arrowheads show nucleolus. Bars = 5 µm. D, Pairwise yeast two-hybrid assays showed that the MiEFF18a and MeEFF18 proteins were able to interact with the SmD1 proteins of *A. thaliana*, *S. lycopersicum* and *N. benthamiana*. We used MiEFF18a and MiEFF16 as a positive and negative control, respectively. Diploid yeasts containing the bait and prey plasmids carrying controls, effectors or SmD1 were serially diluted and spotted on plates. The 10-2 dilution is shown. SD-WL corresponds to the non-selective medium without tryptophan (W) and leucine (L). Only yeasts carrying a protein-protein interaction can survive on the SD-WLH (H, histidine) + 0.5 mM 3-aminotriazole (3-AT) selective medium.

and *NbSmD1c* encode 100% identical protein, and NbSmD1b shares 99.1% with NbSmD1a/c. A multiple sequence alignment showed that SmD1 was highly conserved in these species, with 93% amino acid sequence identity between SlSmD1 and the sequence from which it diverged most strongly, AtSmD1b (Figure 3A). Like all Sm proteins, SmD1s carry two conserved Sm motifs mediating protein-protein interactions during small nuclear ribonucleoprotein (snRNP) biogenesis (Figure 3B). We investigated the subcellular localisation of SmD1 in plant cells, by transiently expressing constructs encoding *GFP-SmD1* fusion proteins in *N. benthamiana*. We confirmed a strong accumulation of NbSmD1b, SlSmD1a and AtSmD1b in the nucleolus and in Cajal bodies, and a weaker accumulation in the nucleoplasm (Figure 3C).

We then investigated whether MeEFF18a was also able to interact with SmD1 proteins from *S.*

lycopersicum and *A. thaliana,* like MiEFF18a (Mejias *et al.*, 2021). Using a pairwise yeast-two hybrid approach, we showed that MiEFF18a and MeEFF18a interact with SmD1 proteins from plants of different clades, such as *A. thaliana*, *S. lycopersicum* and *N. benthamiana* (Figure 3D). As a control, we tested SmD1 interactions with another *M. incognita* effector, MiEFF16, encoded by the *Minc16401* gene and expressed in the subventral glands, with the same nuclear location *in planta* as MiEFF18 (Mejias *et al.*, 2020). No interaction was observed between MiEFF16 and SmD1 proteins in yeast (Figure 3D). These results demonstrate that EFF18 proteins are conserved among RKNs and that they interact with SmD1 proteins, which are conserved among plant species.

M. incognita **triggers alternative splicing in tomato**

To get a deeper insight into the role played by AS in tomato response to *M. incognita*, we analysed paired-end Illumina RNA-seq data of dissected tomato galls 7 and 14 dpi with *M. incognita* and corresponding uninfected roots. The four main categories of AS events, *i.e.* intron retention (IR), exon skipping (ES), alternative 5' splice site (A5) and alternative 3' splice site (A3), were detected, and IR were the most prevalent AS events (Figure 4A; Supplemental Table S3). We identified 583 and 949 differential splicing events in 480 and 717 differentially spliced genes (DSG) in tomato galls at 7 and 14 dpi, respectively (Figure 4A and 4B). To further examine the function of genes undergoing AS, we performed a Gene Ontology (GO) term enrichment analysis. The GO term analysis showed enrichment in genes encoding for proteins associated to nuclear biological processes, with an overrepresentation of genes involved in regulation of histone modification and chromatin organisation, in transcription, and in mRNA transport (Supplemental Table S4). In total, 846 and 2176 differentially expressed genes (DEG) were counted at 7 and 14

A

Alternative splicing events	7 dpi		14 dpi	
	Events	%	Events	%
Intron retention (IR)	279	48	378	40
Exon skipping (ES)	120	21	225	24
Alternative 5' splice site (A5)	72	12	154	16
Alternative 3' splice site (A3)	112	19	192	20
Total:	583	100	949	100

B

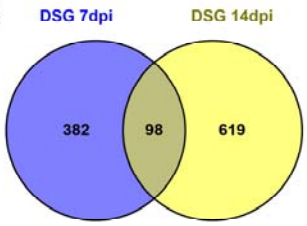

C

7 dpi		14 dpi		Overlapping genes	
up	down	up	down	up	down
487	359	1359	817	337	191

D

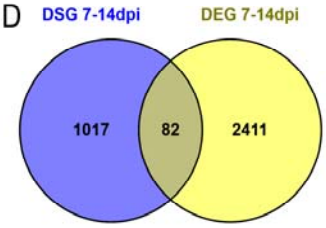

Figure 4. Alternative splicing is triggered in tomato roots upon *M. incognita* infection. A, Tomato genes with alternative splicing events (intron retention, exon skipping, alternative 3' splice site and alternative 5' splice site) in galls 7 and 14 days after inoculation (dpi) with *M. incognita*, relative to uninfected roots. B, Venn diagram showing the overlap between differentially spliced genes (DSG) in *M. incognita*-induced galls at seven and 14 dpi. C, Tomato genes differentially expressed (up or down-regulated) in galls 7 and 14 dpi with *M. incognita*, relative to uninfected roots. D, Venn diagram showing the overlap between differentially spliced genes (DSG) and differentially expressed genes (DEG) in *M. incognita*-induced galls at either 7 or 14 dpi.

dpi, respectively (Figure 4C; Supplemental Table S5 and S6). To determine whether DEG were involved in the same biological processes as DSG, we performed a GO term enrichment analysis. Genes involved in response to the phytohormones auxin and cytokinin, and cell cycle, were overrepresented among the DEG, while genes associated with RNA processing were underrepresented (Supplemental Table S7), demonstrating a distinct function for AS in tomato galls. From the 2493 DEG at either 7 or 14 dpi, 82 genes were also differentially spliced (Figure 4D). Thus, only a small portion of DEGs has splicing defects. These results indicate that AS plays a key role in tomato response to RKN infection, independently of mRNA abundance regulation.

To compare AS patterns induced by *M. incognita* in tomato and *Arabidopsis*, we searched for tomato orthologs of *Arabidopsis* genes alternatively spliced in galls at 5- and/or 7-days post infection with *M. incognita* (Mejias *et al.*, 2021). AS was detected in galls of both species for 40 ortholog pairs (Supplemental Figure S3, Supplemental Table S8), suggesting *M. incognita* could modulate through AS conserved functions in different host species. We also asked whether two

distinct pathogens, *M. incognita* and the oomycete *Phytophthora infestans*, would be responsible for similar AS modulation in tomato. *P. infestans* triggers AS in 2088 genes in tomato (Huang *et al.*, 2020), among which 275 are also differentially spliced upon *M. incognita* infection (Supplemental Table S8). This result indicates that similar responses to different parasites are allowed in tomato by differential splicing on identical targeted genes.

SmD1 acts as a susceptibility gene for infection in plants of different clades

We investigated whether *SmD1* is a conserved susceptibility gene required to ensure infection, and essential for RKN parasitism in Solanaceae species, by using a virus-induced gene silencing (VIGS) approach to alter the expression of *SmD1* genes in *S. lycopersicum* and *N. benthamiana*.

We first performed a VIGS assay to silence *SmD1* genes in *S. lycopersicum* (Figure 5A). According to transcriptomic data gathered on TomExpress, both *SlSmD1a* and *SlSmD1b* are similarly expressed in tomato tissues (Supplemental Figure S4). In addition, according to our RNAseq data, the expression of *SlSmD1a* and *SlSmD1b* did not vary at 7 or 14 dpi with *M. incognita* (Supplemental Table S5 and S6). We evaluated silencing efficiency by RT-qPCR on emerging leaves collected randomly on six independent plants for each treatment. Treated tomatoes had much lower levels of *SmD1* transcripts (Figure 5B). Tomatoes in which SmD1 genes were silenced displayed developmental defects on emerging leaves and had a shorter root system (Supplemental Figure S5 and S6). In tomato plants infected with *M. incognita,* in which *SmD1* genes were silenced, the number of females producing egg masses was much smaller than in control plants treated with the TRV-GFP virus (Figure 5C). The observed decreased susceptibility to nematodes cannot only be explained by the shorter root size, as the calculated number of females producing egg mass per gram of roots is also significantly lower following *SlSmD1* silencing than in the control (Supplemental Figure S6).

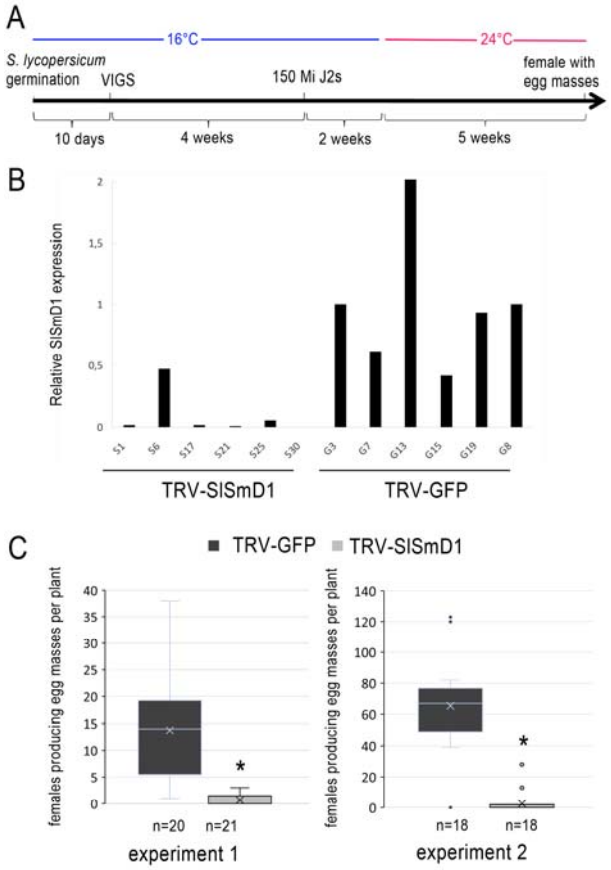

Figure 5 The silencing of *SmD1* genes by VIGS affects susceptibility to *M. incognita* in *S. lycopersicum*. A, Timeline used for the VIGS experiments in S. lycopersicum. B, RT-qPCR demonstrating the effective silencing of *SlSmD1* in TRV-SmD1 line when compared to the control TRV-GFP. *SlRPN7* was used for data normalisation. C, Infection test on tomato plants in which *SlSmD1* genes were silenced (TRV-SmD1) and control tomato plants (TRV-GFP). Females producing egg masses were counted seven weeks after inoculation with 150 *M. incognita* J2s per plant. Boxes indicate interquartile range (25th to the 75th percentile). The central lines within the boxes represent mean values. Whiskers indicate minimum and maximum scores. The crosses represent average values. The circle outside the box represents outlier. Results of two independent replicates are shown. Statistical significance was determined by Kruskal-Wallis tests, and significant differences were observed between TRV-GFP control and TRV-SmD1 plants (*p = 0.01).

Because of the adverse effect of *SmD1* silencing on development in tomato, we then silenced the *SmD1* genes in *N. benthamiana,* which allows performing a VIGS assay at a later developmental stage when roots have already developed substantially (Figure 6A and 6B). An evaluation of silencing efficiency by RT-qPCR showed that *N. benthamiana* roots subjected to VIGS had much lower levels of *NbSmD1b* transcripts than control plants (Figure 6C). We observed no significant expression of *NbSmD1a* and *NbSmD1c* (Figure 6C and Supplemental Figure S7) in non-infected *N. benthamiana* roots. *N. benthamiana* plants in which *NbSmD1b* was

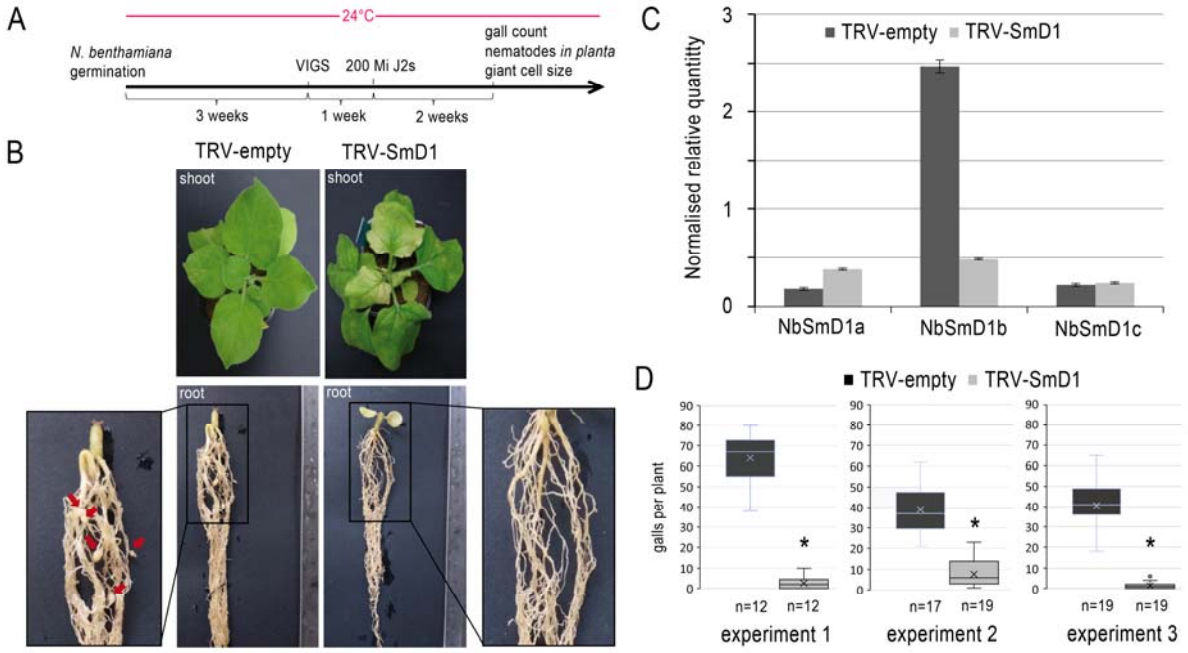

Figure 6 The silencing of *SmD1* genes by VIGS affects susceptibility to *M. incognita* in *N. benthamiana*. A, Timeline used for VIGS experiment in *N. benthamiana*. B, *N. benthamiana* plants with silenced SmD1 genes (TRV-SmD1, right panel) and TRV2-empty control plants (TRV-empty, left panel), showing some developmental defects of the leaves (upper panel) and a shorter root system (lower panel). Red arrow point-out galls on these pictures. C, RT-qPCR showing that the *NbSmD1b* gene, the most strongly expressed and closest orthologue to the *SlSmD1* genes, was effectively silenced. The data shown are the normalized relative transcripts quantities calculated from three independent biological replicates using Qbase. *NbEF1a* and *NbACT1* genes were used for data normalisation. Error bars represent standard deviation. D, Infection test on *N. benthamiana* control plants (TRV-empty) and plants in which *NbSmD1b* was silenced (TRV-SmD1). Galls were counted two weeks after inoculation with 200 *M. incognita* J2s per plant. Boxes indicate interquartile range (25th to the 75th percentile). The central lines within the boxes represent mean values. Whiskers indicate minimum and maximum scores. The crosses represent average values. The circle outside the box represents outlier. Results of three independent replicates are shown. Statistical significance was determined by Kruskal-Wallis tests, and significant differences were observed between TRV-empty control and TRV-SmD1 plants (*p = 0.05; **p = 0.01).

silenced produced a much smaller number of galls (up to 80% fewer) following infection with *M. incognita* (Figure 6D and Supplemental Figure S8). Together these results indicate that *NbSmD1b* gene has a major contribution to the total amount of the SmD1 protein present in *N. benthamiana* roots and to the *N. benthamiana* susceptibility to nematodes.

We studied the effect on nematode and giant cell development in detail, by investigating J2s *in planta* by acid fuchsin staining method, to determine the proportions of migrating filiform and sedentary swollen parasitic juveniles and their ratio. The percentage of migrating filiform J2s was

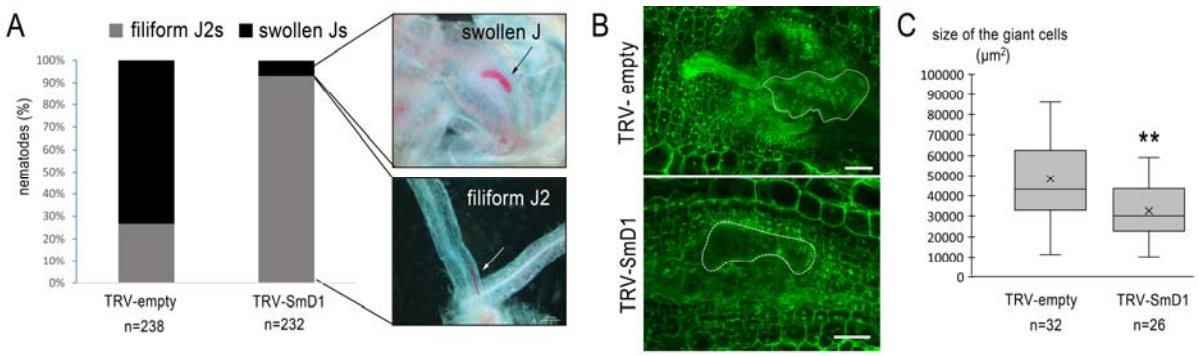

Figure 7 *SmD1* plays an important role in the formation of giant cells. A, The filiform J2s/swollen juveniles (Js) ratio obtained by acid fuchsin staining in the *N. benthamiana* root system with (TRV-SmD1) and without (TRV-empty) silencing with the TRV-SlSmD1 construct, following infection with *M. incognita*. B, Galls of negative control plants and plants with SmD1 silencing collected two weeks post infection for measurement of the area of giant cells (dotted line) by the BABB clearing method (Cabrera et al., 2018). The biggest giant cell measured is shown by a surrounding dashed white line. Bars = 100 µm. C, Box-and-whisker plot of giant cell size (µm2) measurements (n = 32 and 26 galls).

291 higher (90%) in plants in which *SmD1* was silenced, which had a lower percentage of swollen
292 juveniles, indicating a defect in the RKN development (Figure 7A). We also investigated whether
293 the giant cells formed on plants in which *SmD1* was silenced displayed developmental defects. We
294 observed these cells directly, under a confocal microscope, after clearing in benzyl alcohol/benzyl
295 benzoate (BABB ; Cabrera *et al.*, 2018). A comparison of the mean surface areas of the largest
296 giant cells in each gall showed that giant cells from plants in which *SmD1* was silenced were 36%
297 smaller than those from control plants (Figure 7B and 7C). These results confirm the important
298 role of SmD1 in giant cell formation in Solanaceae species and the requirement of this protein for
299 successful nematode development.
300
301

Discussion

The ability of plant pathogens to infect their hosts is generally dependent on the secretion of effectors. Most pathogens secrete effectors to overcome host physical defences, such as the plant cell wall, and to suppress plant immune responses (Toruño *et al.*, 2016). Other effectors are more specific to the parasitic strategy of the pathogen and may regulate host gene expression or trigger changes in host cell morphology and physiology to allow pathogen feeding and development. Most obligatory biotrophs induce specific feeding structures whose formation is allowed by the secretion of specific effectors (Chaudhari *et al.*, 2014; O'Connell and Panstruga, 2006). RKNs are root endoparasites that manipulate host cells to form specialised giant cells for feeding. These giant cells constitute the sole source of nutrients for the nematode, and are, therefore, essential for nematode survival. RKNs induce giant cells by manipulating root cell developmental programmes. Indeed, massive transcriptomic reprogramming occurs during giant cell formation (Favery *et al.*, 2020; Mitchum *et al.*, 2013). Genes associated with root meristem function, lateral root formation and the establishment of the vasculature, in particular, are tightly regulated upon giant cell induction (Cabrera *et al.*, 2014; Olmo *et al.*, 2020; Yamaguchi *et al.*, 2017).

Perturbation of AS is a conserved mechanism involved in RKN disease

In eukaryotes, one gene can produce various mRNA transcripts, causing production of variant proteins, through AS regulation. In plants, AS is a key process in plant development and responses to changing environmental conditions (Reddy *et al.*, 2013; Staiger and Brown, 2013). AS contributes to the regulation of plant-microbe interactions (Rigo *et al.*, 2019), and recent findings indicated a role for AS in *Solanaceae* responses to virus (Zheng *et al.*, 2017a; Zheng *et al.*, 2017b; Zhu *et al.*, 2018), fungi (Tan *et al.*, 2015) and oomycetes (Huang *et al.*, 2020). *Phytophthora*

infestans was shown to trigger differential splicing events in 5125 genes in tomato at either 1, 2 or 3 dpi (Huang *et al.*, 2020). Previously, we reported on the occurrence of AS in Arabidopsis following infection with *M. incognita* contributing to transcriptome and proteome diversity (Mejias *et al.*, 2021). Here, we report differential AS events in 1,099 tomato genes following inoculation with *M. incognita*. Among these genes, 824 were not differentially spliced upon *P. infestans* infection, and most interestingly, only 82 were differentially expressed in galls at either 7 or 14 dpi with *M. incognita*. Thus, AS appears as a specific process, independent from regulation of transcripts abundancy, generally targeted to allow transcriptome reprogramming during plant-RKN interactions.

EFF18 is a nuclear conserved RKN-specific effector

AS regulation by pathogens may be achieved through effectors. *P. infestans* secretes so called splicing regulatory effectors (SREs) able to modulate AS by interfering with splicing factors function (Huang *et al.*, 2020). Similarly, the cyst nematode *Heterodera schachtii* 30D08 effector has been shown to modulate AS when expressed in transgenic Arabidopsis plants, by interacting with the auxiliary spliceosomal protein SMU2 (Verma *et al.*, 2018). MiEFF18 is a RKN effector that has been shown to be secreted within host cells and localises to the nucleus. MiEFF18 has been shown to interact with the SmD1 protein, a core component of the spliceosome conserved in all eukaryotes, thereby modulating alternative splicing and gene expression (Mejias *et al.*, 2021). MiEFF18 may corrupt the function of *Arabidopsis SmD1* function to modulate the expression of various genes encoding proteins involved in giant cell formation through processes such as DNA replication or cytokinesis (Mejias *et al.*, 2021). Here, our RNAseq data indicate hundreds of tomato genes are also differentially spliced in response to RKN, including genes involved in

transcriptional regulation. Thus, modulation of SmD1 function through nematode EFF18 may provide transcriptional control over several genes required for plant development, explaining phenotypes of plants in which *SmD1* genes are silenced, and also for the re-differentiation of root cells into giant feeding cells, in different plant species, including *Nicotiana benthamiana* and the tomato *Solanum lycopersicum.*

Genes encoding the EFF18 effector were found in all available *Meloidogyne* spp. genomes other than the draft genome for the rice RKN *M. graminicola* (Somvanshi *et al.*, 2018). EFF18 is exclusive to RKN, being absent from all other parasitic nematodes and other plant pathogens with parasitic strategies not involving the induction of giant feeding cells. At least one orthologous copy of a MiEFF18a sequence was detected in each of the available *Meloidogyne* genomes, demonstrating that EFF18 is a conserved effector. The multiple copies identified in *M. incognita, M. javanica* and *M. arenaria* are consistent with the polyploidy of these mitotic parthenogenetic species (Koutsovoulos *et al.*, 2020). The absence of EFF18 effector in *M. graminicola* may be explained by its particular host range. *M. graminicola* may have lost the EFF18 when it specialized on monocotyledon hosts. Indeed, *M. graminicola* differs from other *Meloidogyne* species in its life cycle. As an example of adaptation to root submergence, *M. graminicola* females lay eggs inside the root cortex and not on the root surface as other RKNs, to promote J2 survival (Mantelin et al., 2016). One particularity of *M. graminicola* regarding giant cell induction is that the invading larvae will select root cells in the stele at the root tip, close to the root meristem, while other RKNs induce giant cells in an upper part of the vascular cylinder, farther from the root apex (Mantelin et al., 2016). This adaptation may explain a different requirement in modulating genes expression for giant cell ontogenesis, depending on other effector(s) than EFF18. Alternatively, it is possible that the *M. graminicola* genome is still incomplete, such that an EFF18 orthologue has not yet been

identified.

The distribution of EFF18 orthologues in two major groups, with copies (e.g. MiEFF18a) carrying two NLS, and those of the most divergent group (e.g. MiEFF18b) carrying only one NLS, suggested a possible duplication of the ancestral *MiEFF18* gene in the ancestor of RKN species, with one of the duplicated genes either gaining or losing a bipartite NLS. The proteins from the closest group to the *MiEFF18a* gene would be expected to function similarly to MiEFF18a, through the modulation of SmD1 functions, due to the very high level of sequence identity between these proteins (98% identity). *M. enterolobii* is an extremely polyphagous species that reproduces through mitotic parthenogenesis, like *M. incognita*. Therefore, we investigated the functionality of proteins MeEFF18 orthologue. We found that, like MiEFF18a, MeEFF18a was able to interact with SmD1 proteins from *A. thaliana*, *N. benthamiana* and *S. lycopersicum*, suggesting that orthologous copies of MiEFF18a are functional and target the same functions in different host plants. Members of the EFF18 family are the first examples of conserved RKN effectors able to target the same conserved process in different plant species.

Targeting conserved effectors to engineer plant resistance

The identification of conserved effectors could lead to new strategies for developing broad resistance (Huang *et al.*, 2006; Landry *et al.*, 2020; Peeters *et al.*, 2013; Roux *et al.*, 2015). Only a few RKN effectors have been described to be conserved. The MAP (*Meloidogyne* avirulence protein) effector family, which includes *M. incognita* Mi-MAP1.2, was shown to be conserved in 13 of the 21 RKN species tested, and absent from other genera of plant-parasitic nematodes (PPNs) (Tomalova *et al.*, 2012). The genes of the MAP effector family harbour one or multiple CLE-like motifs, which may be involved in feeding site formation, as demonstrated for cyst

nematode CLE-like peptides, which promote syncytium formation (Rutter *et al.*, 2014; Mitchum *et al.*, 2012). MjNULG1a, from *M. javanica,* is a nuclear effector with a demonstrated role in parasitism. Southern blot experiments have revealed the presence of MjNULG1a orthologues in *M. incognita* and *M. enterolobii*, but not in other PPNs (Lin *et al.*, 2013). Similarly, the 16D10 effector is exclusive to RKNs (Huang *et al.*, 2006; Dinh *et al.*, 2014). The use of host-induced gene silencing (HIGS) approaches to engineer plant resistance to RKNs has excited considerable interest (Ali *et al.*, 2017; Banerjee *et al.*, 2017). The targeting of genes involved in nematode development or encoding effectors has been considered. Silencing conserved effectors may allow specific resistance to RKNs with no impact on non-targeted species. Studies of Mi16D10 have demonstrated the feasibility of conferring RKN resistance in *Arabidopsis*, potato or grape through the targeting of this effector (Huang *et al.*, 2006; Yang *et al.*, 2013; Dinh *et al.*, 2014). However, this strategy is constrained both by limited HIGS effectiveness, by the redundancy of the effector's function and the difficulty in targeting the point in time when the effector plays a key role in the interaction.

Targeting essential conserved effector plant targets to induce a loss of susceptibility

The use of resistant cultivars or rootstocks is an efficient and non-polluting method for controlling RKNs. Very few natural resistance genes (R-genes) have been identified to date, in a limited number of plant species. Furthermore, some RKN species or populations are not controlled by these genes, e.g. *M. enterolobii* (Elling, 2013; Kiewnick *et al.*, 2009) or can overcome these resistances, e.g. populations of *M. incognita* virulent against tomato *Mi1.2* (Castagnone-Sereno, 2006). One alternative would be to target conserved plant genes encoding proteins involved in host processes that are hijacked by the biotrophic pathogens for settlement and feeding, and that are

essential for disease development. These susceptibility genes (S-genes) represent an alternative to R-genes for the deployment of pathogen resistance, and they may be more durable in the field (Dong and Ronald, 2019; Engelhardt *et al.*, 2018; van Schie and Takken, 2014). Well-characterised examples of S-genes include the genes encoding eukaryotic translation initiation factors, the sugar transporter SWEET14 or PMR6, which are required for viral, bacterial and oomycete infections, respectively (Langner *et al.*, 2018; van Schie and Takken, 2014; Schmitt-Keichinger, 2019).

In recent decades, transcriptomic approaches have been widely used to identify genes regulated upon RKN infection, and, thus, host functions manipulated by RKNs. However, as thousands of genes are differentially regulated during a compatible interaction, the identification of S-genes from these data is a very time-consuming process, probably explaining why only a few genes to date have been shown to be important for the establishment of giant cells (Favery *et al.*, 2016). Interactomics approaches have recently been used to identify the direct plant targets manipulated by PPN effectors. Only a few targets of RKN effectors have been identified, but most have been shown to be instrumental in promoting nematode parasitism (Mejias *et al.*, 2019). SmD1 is a host target of an effector required for host susceptibility to RKNs in several plant clades. It exerts a conserved plant function targeted by a core effector in *Arabidopsis* and *Solanaceae*, common to diverse *Meloidogyne* species that have adopted the same successful parasitic strategy based on the induction of giant feeding cells in the root in several host species. SmD1 is thus a good candidate S-gene for targeting in the engineering of crop resistance to RKN. As SmD1 function is required for plant development knockout mutations of this gene have adverse effects, it will be necessary to identify mutant alleles that can evade recognition by MiEFF18 whilst remaining competent to perform the functions of SmD1 in the regulation of plant

development in a continually changing environment. This strategy has proven to be effective for potyvirus susceptibility *eIF4E* genes (Bastet *et al.*, 2019). Hence, our work opens wide perspectives for the use of a conserved target involved in AS regulation to develop new strategies for the control of nematode infection.

Experimental procedures

Nematode and plant materials

M. incognita (Morelos strain), *M. arenaria* (Guadeloupe strain) and *M. enterolobii* (Godet strain) were multiplied on tomato (*S. lycopersicum* cv. "Saint Pierre") growing in a growth chamber (25°C, 16 h photoperiod). Freshly hatched J2s were collected as previously described (Caillaud and Favery, 2016).

For VIGS experiments, *N. benthamiana* and *S. lycopersicum* (cv M82) seeds were sown on soil and incubated at 4°C for two days. After germination, *N. benthamiana* and tomato plantlets were transplanted into pots containing soil and sand (1:1), and were grown at 24°C and 16°C, respectively (photoperiod, 16 h: 8 h, light: dark).

For RNAseq analysis, Seeds of *Solanum lycopersicum* cv St Pierre were surface-sterilized with chlorine solution (44% active chlorine) and washed three times with 1ml of milli-Q water. 10 to 15 sterile seeds were sown on a Gamborg B5 (Duchefa Biochemie) agar plates (1x Gamborg B5; pH = 6.4; 1% Sucrose; 0,7% Agar), placed at 24ºC for 48 hours for germination, and finally transferred in a growth chamber (8h light; 16h dark, 20ºC). *M. incognita* strain Morelos" J2s were sterilized with HgCl2 (0.01%) and streptomycin (0.7%) as described before (Caillaud and Favery, 2016). One to two weeks after germination, roots were inoculated with 1,000 sterile J2s resuspended in phytagel (5%) per petri dishes.

463

464 **EFF18 sequence analysis, alignment and phylogenetic tree**

465 The sequences of EFF18 paralogues and orthologues were obtained from *Meloidogyne* genomic
466 resources http://www6.inra.fr/meloidogyne_incognita and Wormbase parasite. Protein sequences
467 were aligned with the MAFFT tool on the EBI server (https://www.ebi.ac.uk/Tools/msa/mafft/).
468 The alignment was then used as input for the IQTree Web server http://iqtree.cibiv.univie.ac.at/
469 (Trifinopoulos *et al.*, 2016) to generate the maximum likelihood phylogenetic tree. The model
470 chosen by the inbuilt model test was HIVb+F+G4. Support for the nodes was calculated with 100
471 bootstrap replicates. *M. hapla* was used as the outgroup in the phylogenetic tree for MiEFF18
472 orthologues. The tree was visualised in iTOL https://itol.embl.de/. The sequence alignment were
473 coloured with Boxshade (https://embnet.vital-it.ch/software/BOX_form.html). The pairwise
474 sequence identity matrix of RKN EFF18 protein sequences was generated with Sequence
475 Demarcation Tool version 1.2 software (Muhire *et al.*, 2014) (http://web.cbio.uct.ac.za/~brejnev/).

476

477 **Cloning of EFF18 effectors**

478 The *MeEFF18a* coding sequence (CDS) lacking the signal peptide was cloned in pDON207 entry
479 vector as described previously for *MiEFF18a* (Mejias *et al.*, 2021) using the MeEFF18_GW3 and
480 MeEFF18_GW5 primers (Supplemental Table S2). *MaEFF18a*, *MiEFF18b* and *MeEFF18c*
481 CDSs were synthesised in pUC57-BsaI-Free entry vector (Gene Universal INC., USA).

482

483 ***In situ* hybridisation (ISH)**

484 ISH was performed on freshly hatched *M. arenaria* and *M. enterolobii* pre-J2s, as previously
485 described (Jaouannet *et al.*, 2018). For probes production, the *MaEFF18a*, and *MeEFF18a*
486 specific sequences were amplified from entry vectors with the same primers (EFF18_F and

MeEFF18_GW5; Supplemental Table S2). Sense probes for MaEFF18 and MeEFF18 were used as negative controls. Images were obtained with a microscope (Zeiss Axioplan2, Germany).

Pairwise yeast two-hybrid assays

For pairwise yeast two-hybrid (Y2H) assays, the coding sequences (CDS) of the MiEFF16 MiEFF18a and MeEFF18a were amplified (Supplemental Table S2) and inserted into pB27 as C-terminal fusions with LexA. Full-length SmD1 CDS sequences (*SlSmD1*, *NbSmD1b* and *AtSmD1b*) were amplified (Supplemental Table S2) and inserted into pP6 as C-terminal fusions with Gal4-AD. The pB27 and pP6 constructs were verified by sequencing and used to transform the L40ΔGal4 (MATa) and Y187 (MATα) yeast strains, respectively. Y187 and L40ΔGal4 were crossed and diploids were selected on medium lacking tryptophan and leucine. Interactions were investigated on medium lacking tryptophan, leucine and histidine and supplemented with 0.5 mM 3-aminotriazole (3-AT).

***N. benthamiana* agroinfiltration**

EFF18s, without the sequences corresponding to their signal peptide for secretion, were cloned into the pK7FWG2 binary vector (Karimi et al. 2002). Transient expression was achieved by infiltrating *N. benthamiana* leaves with *Agrobacterium tumefaciens* GV3101 strains harbouring GFP-fusions, as previously described (Caillaud *et al.*, 2008). Leaves were imaged 48 hours after agroinfiltration, with an inverted confocal microscope equipped with an argon ion and HeNe laser as the excitation source. For simultaneous GFP imaging, samples were excited at 488 nm and GFP emission was detected selectively with a 505-530 nm band-pass emission filter.

Virus-induced gene silencing in Solanaceae

VIGS assays were performed on *N. benthamiana* and *S. lycopersicum*. We used the Sol Genomics Network VIGS-Tool (https://vigs.solgenomics.net/) to design the best sequence for silencing SmD1 transcripts in both *Solanaceae*. Because nucleotide sequences for *SlSmD1a*, *SlSmD1b* and *NbSmD1b* are so similar (Supplemental Figure S9), we selected the full-length *SlSmD1a* (without the ATG and STOP codons) for amplification by PCR with the TRV2-SlSmD1-F/TRV2-SlSmD1-R primer pairs (Supplemental Table S2). The PCR products were digested with *Eco*RI and *Xho*I and ligated to the tobacco rattle virus RNA 2 vector (TRV2) for the transformation of *A. tumefaciens* strain GV3101. VIGS assays were performed, as previously described, by the co-infiltration of leaves of three-week-old *N. benthamiana* plants (Lange *et al.*, 2013; Velasquez *et al.*, 2009) or 10-days-old tomato plants (Cox *et al.*, 2019) with agrobacterial strains containing the RNA 1 vector (TRV1) and TRV2. Tomato plants were incubated at 16°C for four weeks. Three independent biological replicates were established for each set of conditions (n = 15 to 21 per replicate). Leaves from six *S. lycopersicum* leaves per condition were randomly collected upon RKN infection and frozen in liquid nitrogen for subsequent RNA extraction and the assessment of silencing efficiency by RT-qPCR. To validate silencing efficiency in *N. benthamiana* by RT-qPCR, two root systems per set of conditions and per replicate were collected upon RKN infection and frozen in liquid nitrogen for subsequent RNA extraction.

Reverse transcription-quantitative PCR

We assessed silencing efficiency in *Solanaceae* species, by extracting total RNA with TriZol (Invitrogen) and subjecting 1 µg of total RNA to reverse transcription with the Superscript IV

reverse transcriptase (Invitrogen). For performing RT-qPCR on tomato, primers were designed to amplify both *SlSmD1* transcripts (Supplemental Table S2). *SlRNP7* was used for normalization and qPCR analyses were performed with Qbase (Hellemans et al., 2007). The expression level in one of the control plants infiltrated with agrobacteria carrying the TRV2-GFP construct was set to 1. RT-qPCR analyses on *N. benthamiana* samples were performed with the primers described in Supplemental Table S2. To discriminate between the three copies of *SmD1* present in *N. benthamiana* specifically and to prevent the amplification of TRV2-SlSmD1 construct, primers were designed according to their UTRs. *NbEF1a* and *NbACT1* were used for the normalization of RT-qPCR data (Liu et al., 2012). Three technical replicates for three independent biological experiments were performed, and data are presented as Normalized Relative Quantity with Standard Deviation generated using qBase software (Hellemans et al., 2007).

RKN infection assay, juveniles in the plant and giant cell area measurements

N. benthamiana plants subjected to VIGS were inoculated with 200 *M. incognita* J2s per plant, 10 days post inoculation (dpi) with TRV, and incubated at 24°C. *S. lycopersicum* plants subjected to VIGS were inoculated with 150 *M. incognita* J2s per plant, 30 dpi with TRV, and incubated at 16°C for two weeks before transfer to 24°C. *N. benthamiana* infected roots were collected two weeks after infection whereas *S. lycopersicum* infected roots were collected six weeks after infection. Galls or egg masses stained with 4.5% eosin were counted under a binocular microscope, and root system was weighted (n=12 to 19 and n=18 to 21 plants per replicates for *N. benthamiana* and *S. lycopersicum*, respectively). Three and two independent biological replicates were established for each set of conditions in *N. benthamiana* and *S. lycopersicum*, respectively. The impact of the plant lines on the number of galls per mg of root in *N. benthamiana* and the

number of egg masses per plant in *S. lycopersicum* were analyzed using Kruskal Wallis test since the dependent variable did not follow a Normal distribution using a Shapiro-Wilk Test. The different replicates of the numbers of galls per mg of roots in *N. benthamiana* were pooled for the analyzes because there was no difference between the replications (X^2_2= 2.8, P = 0.248). By contrast, the different replicates of the number of egg masses per plant in *S. lycopersicum* varied depending on the replication (X^2_1= 5.3, P = 0.022), and they were analyzed separately. Thus, both the number of galls per mg of root in *N. benthamiana* and the number of egg masses per plant in *S. lycopersicum* varied significantly between the two plant lines tested (X^2_1= 57.2, $P < 0.001$; $X^2_1 >$ 25.6, $P < 0.001$, respectively). For determination of the ratio of filiform-to-swollen nematodes, infected roots were collected 14 dpi, parasitic nematodes were stained with acid fuchsin, as previously described (Karssen and Moens, 1983), and nematodes were examined under a binocular microscope (model LSM 880; Zeiss) (n= 3 plants per replicate for TRV-empty lines and n = 5 plants per replicate for TRV-SmD1 lines, with a mean of 75 nematodes observed per condition and per replicate). Three independent biological replicates were established for each set of conditions. Statistical analyses were carried out with R software (R Development Core Team, version 3.1.3). For giant cell area measurements, galls were cleared in BABB, as previously described (Cabrera *et al.*, 2018), and examined under an inverted confocal microscope (model LSM 880; Zeiss). The mean areas of the biggest giant cell in each gall from *N. benthamiana*, for each genotype, were measured with Zeiss ZEN software (n = 32 and 26 galls for control and SmD1-VIGSed plants, respectively). One biological experiment was performed for giant cells measurement. The data were analysed with a *t*-test since the data followed a normal distribution (t = 3.5, $P < 0.001$).

RNA extraction and sequencing

Total RNAs, including small RNAs (< 200 nt), were isolated from *in vitro* galls or uninfected roots at 7 and 14 dpi. Approximately 40 galls or uninfected roots devoid meristems were independently frozen into powder by using a tissue lyser (Retsch; MM301) at 30 Hertz frequency for 30 seconds with 4 mm tungsten balls (Retsch; MM301). Total RNAs were extracted from these samples with the miRNeasy Mini Kit (Qiagen), according to the manufacturer's instructions, with three additional washes in RPE buffer. PolyA-RNA libraries were generated from 500 ng of total RNA using Truseq Stranded mRNA kit (Illumina). Libraries were then quantified with Qubit dsDNA High Sensitivity Assay Kit (Invitrogen) and pooled. 4nM of this pool were loaded on a Nextseq 500 High output Flowcell and sequenced on a NextSeq 500 platform (Illumina) with 2×75bp paired-end chemistry. These sequencing data have been referenced in the SRA database under the accession PRJNA799360.

Gene expression and alternative splicing analysis

RNA-seq preprocessing included trimming library adapters and quality controls with Trimmomatic using the following arguments; TrimmomaticPE - LEADING:25 TRAILING:25 CROP:120 MINLEN:120. Illumina adapters were removed and read pairs were trimmed to the same length. Processed reads were aligned using STAR with the following arguments: --outSAMtype BAM SortedByCoordinate --outReadsUnmapped Fastx --readFilesCommand zcat, --quantMode GeneCounts, --outFilterMultimapNmax 1. Reads overlappings exons per genes were counted using the FeatureCounts function of the Rsubreads package using the previously published GTF annotation files. Significance of differential gene expression was estimated using DEseq2, and the FDR correction of the p-value was used during pairwise comparison between genotypes. A gene was declared differentially expressed if its adjusted p-value (FDR) was ≤ 0.01. De novo transcript prediction was

made using Stringtie with the following setting --rf -c 2.5 -j 10 one each separated sample. Transcript annotations were merge using Stringtie --merge with the following options -F 0 -T 0 -c 0. New transcript isoforms were added the tomato ITAGv3.2 genome annotation. Differential splicing was determined using our extended transcript annotation using rMATS v4.02 (http://rnaseq-mats.sourceforge.net/) with the following arguments -nthread 4 --readLength 120 -t paired --libType fr-firststrand. Events with FDR <0.01 and |IncLevelDifference|>0.2 were defined as differentially alternatively spliced. GO term enrichments were analyzed using PANTHER16.0 (http://geneontology.org/). Comparison of DSG between tomato and *Arabidopsis* was done using an Orthology analysis. *Arabidopsis* orthologous genes of tomato DAS genes were retrieved from the Ensembl BioMart repository (https://www.ensembl.org/info/genome/compara/homology_types.html). The list of DSG from tomato challenged with *Phytophthora infestans* was extracted from the analysis of Huang *et al.* (2020). DSG in tomato leaves at 1, 2 or 3 days post inoculation with *P. infestans* were retained in our analysis.

Graphs and statistical analysis

Graphs and plots were created with Microsoft® Office Excel® 2016. Venn diagrams were produced with Venny 2.1.0 (https://bioinfogp.cnb.csic.es/tools/venny/). Statistical calculations were performed in R.

Accession numbers

The sequence data from this article can be found in the *Arabidopsis* Information Resource (https://www.arabidopsis.org/), Solgenomics (https://solgenomics.net/) and/or GenBank/EMBL databases. All RKN EFF18 protein sequences are presented in the Figure S1 The accession

numbers are summarised in Table S1 including MiEFF18a (KX907770), MeEFF18a (MW272456), NbSmD1a (MT683762), NbSmD1b (MT683763) and NbSmD1c (MT683764). RNAseq data have been referenced in the SRA database under the accession PRJNA799360.

Acknowledgements

We thank Dr Johnathan Dalzell and Steven Dyer (Queen's University Belfast, UK) for tomato VIGS protocol and vectors, Pr S.P. Dinesh-Kumar (University of California, Davis, USA) for VIGS vectors and Hybrigenics Services (Paris, France) for providing the pB27 and pP6 vectors and the L40ΔGal4 and Y187 yeast strains. We thank Dr Nemo Peeters and Dr Laurent Deslandes (LIPM, Castanet Tolosan, France) and Gregori Bonnet (Syngenta seeds) for helpful discussions. Microscopy work was performed at the SPIBOC imaging facility of Institut Sophia Agrobiotech. We thank Dr Lucie S. Monticelli for helping with the statistical analyses. We thank Dr Olivier Pierre and the whole platform team for their help with microscopy. This work was funded by the INRAE SPE department and the French Government (National Research Agency, ANR) through the 'Investments for the Future' LabEx SIGNALIFE: programme reference #ANR-11-LABX-0028-01, by the INRA-Syngenta Targetome project, by the French-Japanese bilateral collaboration programmes PHC SAKURA 2016 #35891VD and 2019 #43006VJ and by the French-Chinese bilateral collaboration program PHC XU GUANGQI 2020 #45478PF. This work was also supported the "Laboratoire d'Excellence (LABEX)" Saclay Plant Sciences (SPS; ANR-10-LABX-40). J.M. held a doctoral fellowship from the French *Ministère de l'Enseignement Supérieur, de la Recherche et de l'Innovation* (MENRT grant). N.M.T. was supported by a USTH fellowship, as part of the 911-USTH programme of the Ministry of Education and Training of The Socialist Republic of Vietnam. Y.C. obtained scholarships from the

China Scholarship Council (No. 201806350108) for studies at INRAE, France.

Figure legends

Figure 1 Effector 18 (EFF18) is a conserved effector in root-knot nematodes. A, Phylogenetic tree and schematic diagram of root-knot nematode EFF18 protein sequences. The tree scale corresponds to the number of substitutions per site based on the amino-acid matrix (JTT). In the schematic diagram of EFF18 proteins, the predicted secretion signal peptide (SP; grey boxes), the aspartic acid and glutamic acid (D-E)-rich region (red boxes), the lysine (K)–rich C-terminal region (blue boxes) and the nuclear mono- (purple boxes) or bi- (orange boxes) partite localisation signals (NLS) are shown. EFF18 proteins from the closest group to MiEFF18a carry one mono- and one bipartite NLS, whereas the most divergent copies have only a single monopartite NLS. B, Pairwise sequence identity matrix for RKN EFF18 protein sequences. C, EFF18 localised to the nucleus and nucleolus of plant cells. The MiEFF18s, MaEFF18a and MeEFF18a sequences were fused to that encoding GFP in a C-terminal position and expressed in *N. benthamiana* leaves by agroinfiltration. GFP was used as a control and gave fluorescence in the cytoplasm and the nucleus (n), but not the nucleolus (arrowhead). Bars = 10 µm.

Figure 2 RKN EFF18s are specifically expressed in the subventral glands. *In situ* hybridisation, showing EFF18 transcripts in the subventral glands of J2s of *M. arenaria* and *M. enterolobii*. Sense probes for the *MaEFF18* and *MeEFF18* transcripts were used as a negative control. SvG, subventral glands. Bars = 40 µm.

Figure 3 Conserved SmD1 proteins are targeted by EFF18. A, MAFFT protein sequence

674 alignment of the *S. lycopersicum* (Sl), *N. benthamiana* (Nb) and *A. thaliana* (At) SmD1 proteins.
675 B, Schematic representation of Sm1 and Sm2 motif in SmD1 proteins. C, GFP-AtSmD1b,
676 GFP-SlSmD1a and GFP-NbSmD1b accumulate in the nucleus and particularly in the nucleolus
677 when transiently expressed in *N. benthamiana* epidermal leaf cells. GFP was used as a
678 nucleocytoplasmic control. n= nucleoplasm; White arrowheads show nucleolus. Bars = 5 µm. D,
679 Pairwise yeast two-hybrid assays showed that the MiEFF18a and MeEFF18 proteins were able to
680 interact with the SmD1 proteins of *A. thaliana*, *S. lycopersicum* and *N. benthamiana*. We used
681 MiEFF18a and MiEFF16 as a positive and negative control, respectively. Diploid yeasts
682 containing the bait and prey plasmids carrying controls, effectors or SmD1 were serially diluted
683 and spotted on plates. The 10-2 dilution is shown. SD-WL corresponds to the non-selective
684 medium without tryptophan (W) and leucine (L). Only yeasts carrying a protein-protein
685 interaction can survive on the SD-WLH (H, histidine) + 0.5 mM 3-aminotriazole (3-AT) selective
686 medium.
687
688 **Figure 4.** Alternative splicing is triggered in tomato roots upon *M. incognita* infection. A, Tomato
689 genes with alternative splicing events (intron retention, exon skipping, alternative 3' splice site and
690 alternative 5' splice site) in galls 7 and 14 days after inoculation (dpi) with *M. incognita,* relative to
691 uninfected roots. B, Venn diagram showing the overlap between differentially spliced genes
692 (DSG) in *M. incognita*-induced galls at seven and 14 dpi. C, Tomato genes differentially expressed
693 (up or down-regulated) in galls 7 and 14 dpi with *M. incognita*, relative to uninfected roots. D,
694 Venn diagram showing the overlap between differentially spliced genes (DSG) and differentially
695 expressed genes (DEG) in *M. incognita*-induced galls at either 7 or 14 dpi.
696

Figure 5 The silencing of *SmD1* genes by VIGS affects susceptibility to *M. incognita* in *S. lycopersicum*. A, Timeline used for the VIGS experiments in S. lycopersicum. B, RT-qPCR demonstrating the effective silencing of *SlSmD1* in TRV-SmD1 line when compared to the control TRV-GFP. *SlRPN7* was used for data normalisation. C, Infection test on tomato plants in which *SlSmD1* genes were silenced (TRV-SmD1) and control tomato plants (TRV-GFP). Females producing egg masses were counted seven weeks after inoculation with 150 *M. incognita* J2s per plant. Boxes indicate interquartile range (25th to the 75th percentile). The central lines within the boxes represent mean values. Whiskers indicate minimum and maximum scores. The crosses represent average values. The circle outside the box represents outlier. Results of two independent replicates are shown. Statistical significance was determined by Kruskal-Wallis tests, and significant differences were observed between TRV-GFP control and TRV-SmD1 plants (*$p \leq 0.01$).

Figure 6 The silencing of *SmD1* genes by VIGS affects susceptibility to *M. incognita* in *N. benthamiana*. A, Timeline used for VIGS experiment in *N. benthamiana*. B, *N. benthamiana* plants with silenced SmD1 genes (TRV-SmD1, right panel) and TRV2-empty control plants (TRV-empty, left panel), showing some developmental defects of the leaves (upper panel) and a shorter root system (lower panel). Red arrow point-out galls on these pictures. C, RT-qPCR showing that the *NbSmD1b* gene, the most strongly expressed and closest orthologue to the *SlSmD1* genes, was effectively silenced. The data shown are the normalized relative transcripts quantities calculated from three independent biological replicates using Qbase. *NbEF1a* and *NbACT1* genes were used for data normalisation. Error bars represent standard deviation. D, Infection test on *N. benthamiana* control plants (TRV-empty) and plants in which *NbSmD1b* was

720 silenced (TRV-SmD1). Galls were counted two weeks after inoculation with 200 *M. incognita* J2s
721 per plant. Boxes indicate interquartile range (25th to the 75th percentile). The central lines within
722 the boxes represent mean values. Whiskers indicate minimum and maximum scores. The crosses
723 represent average values. The circle outside the box represents outlier. Results of three
724 independent replicates are shown. Statistical significance was determined by Kruskal-Wallis tests,
725 and significant differences were observed between TRV-empty control and TRV-SmD1 plants (*p
726 ≤ 0.05; **p ≤ 0.01).
727
728 **Figure 7** *SmD1* plays an important role in the formation of giant cells. A, The filiform J2s/swollen
729 juveniles (Js) ratio obtained by acid fuchsin staining in the *N. benthamiana* root system with
730 (TRV-SmD1) and without (TRV-empty) silencing with the TRV-SlSmD1 construct, following
731 infection with *M. incognita*. B, Galls of negative control plants and plants with SmD1 silencing
732 collected two weeks post infection for measurement of the area of giant cells (dotted line) by the
733 BABB clearing method (Cabrera et al., 2018). The biggest giant cell measured is shown by a
734 surrounding dashed white line. Bar = 100 µm. C, Box-and-whisker plot of giant cell size (µm2)
735 measurements (n = 32 and 26 galls).
736
737 **Supplementary informations**
738 **Figure S1** Identified EFF18 sequences in RKN species.
739 **Figure S2** EFF18 is a conserved RKN effector.
740 **Figure S3** *M. incognita* triggers alternative splicing in orthologous genes in Arabidopsis and
741 tomato.
742 **Figure S4** *SlSmD1a* and *SlSmD1b* are similarly expressed in tomato tissues.
743 **Figure S5** Tomato phenotypes associated with VIGS of *SlSmD1* genes.

744 **Figure S6** Silencing *SmD1* genes in tomato affects both root develpment and *M. incognita*
745 parasitism.
746 **Figure S7** Semi-quantitative RT-PCR expression analysis of *NbSmD1* transcripts in *N.*
747 *benthamiana* VIGS experiments.
748 **Figure S8** Silencing *SmD1* genes in *Nicotiana benthamiana* affects both root development and *M.*
749 *incognita* parasitism.
750 **Figure S9** Nucleotide sequences of *SlSmD1a*, *SlSmD1b* and *NbSmD1b* are highly identical.
751 **Table S1** Sequences used in this study and accession numbers.
752 **Table S2** Primers used in this study.
753 **Table S3** Altered splicing events identified in *Solanum lycopersicum* at 7 and 14 dpi with
754 *Meloidogyne incognita.*
755 **Table S4** GO term enrichment in DSG
756 **Table S5** Differentially expressed genes identified in *Solanum lycopersicum* at 7 dpi with
757 *Meloidogyne incognita.*
758 **Table S6** Differentially expressed genes identified in *Solanum lycopersicum* at 14dpi with
759 *Meloidogyne incognita.*
760 **Table S7** GO term enrichment in DEG.
761 **Table S8** Comparison of differentially expressed genes identidied in tomato and *Arabidopsis* galls
762 and tomato leaves inoculated with *Phytophthora infestans*.
763
764
765

Parsed Citations

Ali, M.A., Azeem, F., Abbas, A., Joyia, F.A., Li, H., and Dababat, A.A. (2017) Transgenic strategies for enhancement of nematode resistance in plants. Frontiers in Plant Science, 8, 1–13.
Google Scholar: Author Only Title Only Author and Title

de Almeida Engler, J. and Gheysen, G. (2013) Nematode-induced endoreduplication in plant host cells: why and how? Molecular Plant-Microbe Interactions, 26, 17–24.
Google Scholar: Author Only Title Only Author and Title

Banerjee, S., Banerjee, A., Gill, S.S., Gupta, O.P., Dahuja, A., Jain, P.K., and Sirohi, A. (2017) RNA interference: a novel source of resistance to combat plant parasitic nematodes. Frontiers in Plant Science, 8:834, doi: 10.3389/fpls.2017.00834.
Google Scholar: Author Only Title Only Author and Title

Bastet, A., Zafirov, D., Giovinazzo, N., Guyon-Debast, A., Nogué, F., Robaglia, C., and Gallois, J.L. (2019) Mimicking natural polymorphism in eIF4E by CRISPR-Cas9 base editing is associated with resistance to potyviruses. Plant Biotechnology Journal, 17, 1736–1750.
Google Scholar: Author Only Title Only Author and Title

Blanc-Mathieu, R., Perfus-Barbeoch, L., Aury, J.-M.M., Da Rocha, M., Gouzy, J., Sallet, E., et al. (2017) Hybridization and polyploidy enable genomic plasticity without sex in the most devastating plant-parasitic nematodes. PLoS Genetics, 13, e1006777.
Google Scholar: Author Only Title Only Author and Title

Blok, V.C., Jones, J.T., Phillips, M.S., and Trudgill, D.L. (2008) Parasitism genes and host range disparities in biotrophic nematodes: the conundrum of polyphagy versus specialisation. Bioessays, 30, 249–259.
Google Scholar: Author Only Title Only Author and Title

Cabrera, J., Bustos, R., Favery, B., Fenoll, C., and Escobar, C. (2014) NEMATIC: a simple and versatile tool for the in silico analysis of plant-nematode interactions. Molecular Plant Pathology, 15, 627–636.
Google Scholar: Author Only Title Only Author and Title

Cabrera, J., Olmo, R., Ruiz-Ferrer, V., Abreu, I., Hermans, C., Martinez-Argudo, I., et al. (2018) A phenotyping method of giant cells from root-knot nematode feeding sites by confocal microscopy highlights a role for CHITINASE-LIKE 1 in Arabidopsis. International Journal of Molecular Sciences, 19, 429.
Google Scholar: Author Only Title Only Author and Title

Caillaud, M.-C., Abad, P., and Favery, B. (2008) Cytoskeleton reorganization. Plant Signaling & Behavior, 3, 816–818.
Google Scholar: Author Only Title Only Author and Title

Caillaud, M.-C.C. and Favery, B. (2016) In vivo imaging of microtubule organization in dividing giant cell. In: Methods in Molecular Biology (Caillaud,M.-C., ed) , pp. 137–144. New York: Springer New York.
Google Scholar: Author Only Title Only Author and Title

Castagnone-Sereno, P. (2006) Genetic variability and adaptive evolution in parthenogenetic root-knot nematodes. Heredity, 96, 282–289.
Google Scholar: Author Only Title Only Author and Title

Chaudhari, P., Ahmed, B., Joly, D.L., and Germain, H. (2014) Effector biology during biotrophic invasion of plant cells. Virulence, 5, 703–709.
Google Scholar: Author Only Title Only Author and Title

Cox, D.E., Dyer, S., Weir, R., Cheseto, X., Sturrock, M., Coyne, D., et al. (2019) ABC transporter genes ABC-C6 and ABC-G33 alter plant-microbe-parasite interactions in the rhizosphere. Scientific Reports, 9, 19899.
Google Scholar: Author Only Title Only Author and Title

Danchin, E.G.J., Rosso, M.-N.N., Vieira, P., de Almeida-Engler, J., Coutinho, P.M., Henrissat, B. and Abad, P. (2010) Multiple lateral gene transfers and duplications have promoted plant parasitism ability in nematodes. Proc Natl Acad Sci U S A, 107, 17651–17656.
Google Scholar: Author Only Title Only Author and Title

Dinh, P.T.Y. , Brown, C.R. and Elling, A.A. (2014) RNA interference of effector gene Mc16D10L confers resistance against Meloidogyne chitwoodi in Arabidopsis and potato. Nematology, 104, 1098–1106.
Google Scholar: Author Only Title Only Author and Title

Dong, O.X. and Ronald, P.C. (2019) Genetic engineering for disease resistance in plants: recent progress and future perspectives. Plant Physiology, 180, 26–38.
Google Scholar: Author Only Title Only Author and Title

Doyle, E.A. and Lambert, K.N. (2003) Meloidogyne javanica chorismate mutase 1 alters plant cell development. Molecular Plant-Microbe Interactions, 16, 123–131.
Google Scholar: Author Only Title Only Author and Title

Elling, A.A. (2013) Major emerging problems with minor meloidogyne species. Phytopathology, 103, 1092–1102.
Google Scholar: Author Only Title Only Author and Title

Engelhardt, S., Stam, R., and Hückelhoven, R. (2018) Good riddance? Breaking disease susceptibility in the era of new breeding technologies. Agronomy, 8, 114.
Google Scholar: Author Only Title Only Author and Title

Escobar, C., Barcala, M., Cabrera, J., and Fenoll, C. (2015) Overview of root-knot nematodes and giant cells. Advances in Botanical Research , 73, 1–32.
Google Scholar: Author Only Title Only Author and Title

Favery, B., Dubreuil, G., Chen, M.S., Giron, D. and Abad, P. (2020) Gall-inducing parasites: convergent and conserved strategies of plant manipulation by insects and nematodes. Annual Review of Phytopathology, 58, 1-22.
Google Scholar: Author Only Title Only Author and Title

Favery, B., Quentin, M., Jaubert-Possamai, S., and Abad, P. (2016) Gall-forming root-knot nematodes hijack key plant cellular functions to induce multinucleate and hypertrophied feeding cells. Journal of Insect Physiology, 84, 60–69.
Google Scholar: Author Only Title Only Author and Title

Gleason, C., Polzin, F., Habash, S.S., Zhang, L., Utermark, J., Grundler, F.M.W., and Elashry, A. (2017) Identification of two Meloidogyne hapla genes and an investigation of their roles in the plant-nematode interaction. Molecular Plant-Microbe Interactions, 30, 101–112.
Google Scholar: Author Only Title Only Author and Title

Hellemans, J., Mortier, G., De Paepe, A., Speleman, F., and Vandesompele, J. (2007). qBase relative quantification framework and software for management and automated analysis of real-time quantitative PCR data. Genome Biology, 8, 1–14.
Google Scholar: Author Only Title Only Author and Title

Hewezi, T. and Baum, T.J. (2013) Manipulation of plant cells by cyst and root-knot nematode effectors. Molecular Plant-Microbe Interactions, 26, 9–16.
Google Scholar: Author Only Title Only Author and Title

Holbein, J., Franke, R.B., Marhavý, P., Fujita, S., Górecka, M., Sobczak, M., et al. (2019) Root endodermal barrier system contributes to defence against plant-parasitic cyst and root-knot nematodes. The Plant Journal, 100, 221–236.
Google Scholar: Author Only Title Only Author and Title

Huang, G.Z., Allen, R., Davis, E.L., Baum, T.J., and Hussey, R.S. (2006) Engineering broad root-knot resistance in transgenic plants by RNAi silencing of a conserved and essential root-knot nematode parasitism gene. Proceedings of the National Academy of Sciences of the United States of America, 103, 14302–14306.
Google Scholar: Author Only Title Only Author and Title

Huang, J., Lu, X., Wu, H., Xie, Y., Peng, Q., Gu, L., Wu, J., Wang, Y., Reddy, A.S.N. and Dong, S. (2020) Phytophthora effectors modulate genome-wide alternative splicing of host mRNAs to reprogram plant immunity, Molecular Plant, 13, 1470-1484.
Google Scholar: Author Only Title Only Author and Title

Jaouannet, M., Nguyen, C.-N., Quentin, M., Jaubert-Possamai, S., Rosso, M.-N., and Favery, B. (2018) In situ hybridization (ISH) in preparasitic and parasitic stages of the plant-parasitic nematode Meloidogyne spp. Bio-Protocol, 8, 1–13.
Google Scholar: Author Only Title Only Author and Title

Jones, J.T., Haegeman, A., Danchin, E.G.J.J., Gaur, H.S., Helder, J., Jones, M.G.K.K., et al. (2013) Top 10 plant-parasitic nematodes in molecular plant pathology. Molecular Plant Pathology, 14, 946–961.
Google Scholar: Author Only Title Only Author and Title

Karimi, M., Inzé, D. and Depicker, A. (2002) GATEWAYTM vectors for Agrobacterium-mediated plant transformation. Trends in Plant Science, 7, 193–195.
Google Scholar: Author Only Title Only Author and Title

Karssen, G. and Moens, M. (1983) Root-knot nematodes. In: Plant nematology , pp. 59–90. Wallingford: CABI.
Google Scholar: Author Only Title Only Author and Title

Kiewnick, S., Dessimoz, M., and Franck, L. (2009) Effects of the Mi-1 and the N root-knot nematode-resistance gene on infection and reproduction of Meloidogyne enterolobii on tomato and pepper cultivars. Journal of nematology, 41, 134–9.
Google Scholar: Author Only Title Only Author and Title

Koutsovoulos, G.D., Poullet, M., Elashry, A., Kozlowski, D.K.L., Sallet, E., Da Rocha, M., et al. (2020) Genome assembly and annotation of Meloidogyne enterolobii, an emerging parthenogenetic root-knot nematode. Scientific Data, 7, 324.
Google Scholar: Author Only Title Only Author and Title

Landry, D., González-Fuente, M., Deslandes, L., and Peeters, N. (2020) The large, diverse, and robust arsenal of Ralstonia solanacearum type III effectors and their in planta functions. Molecular Plant Pathology, 21, 1377–1388.

Google Scholar: Author Only Title Only Author and Title

Lange, M., Yellina, A.L., Orashakova, S., and Becker, A. (2013) Virus-induced gene silencing (VIGS) in plants: an overview of target species and the virus-derived vector systems. In: Methods in Molecular Biology , pp. 1–14. Humana Press Inc.
Google Scholar: Author Only Title Only Author and Title

Langner, T., Kamoun, S., and Belhaj, K. (2018) CRISPR crops: plant genome editing toward disease resistance. Annual Review of Phytopathology, 56, 479–512.
Google Scholar: Author Only Title Only Author and Title

Lin, B., Zhuo, K., Chen, S., Hu, L., Sun, L., Wang, X., et al. (2016) A novel nematode effector suppresses plant immunity by activating host reactive oxygen species-scavenging system. New Phytologist, 209, 1159–1173.
Google Scholar: Author Only Title Only Author and Title

Lin, B., Zhuo, K., Wu, P., Cui, R., Zhang, L.-H., and Liao, J. (2013) A novel effector protein, MJ-NULG1a, targeted to giant cell nuclei plays a role in Meloidogyne javanica parasitism. Molecular plant-microbe interactions, 26, 55–66.
Google Scholar: Author Only Title Only Author and Title

Liu, D., Shi, L., Han, C., Yu, J., Li, D., and Zhang, Y. (2012) Validation of reference genes for gene expression studies in virus-infected Nicotiana benthamiana using quantitative real-time PCR. PLoS ONE, 7, e46451.
Google Scholar: Author Only Title Only Author and Title

Lunt, D.H., Kumar, S., Koutsovoulos, G., and Blaxter, M.L. (2014) The complex hybrid origins of the root knot nematodes revealed through comparative genomics. PeerJ, 2, e356.
Google Scholar: Author Only Title Only Author and Title

Mantelin, S., Bellafiore, S., and Kyndt, T. (2017) Meloidogyne graminicola : a major threat to rice agriculture. Molecular Plant Pathology, 18, 3–15.
Google Scholar: Author Only Title Only Author and Title

Mejias, J., Bazin, J., Truong, N., Chen, Y., Marteu, N., Bouteiller, N., et al. (2021) The root-knot nematode effector MiEFF18 interacts with the plant core spliceosomal protein SmD1 required for giant cell formation. New Phytologist, 229, 3408–3423.
Google Scholar: Author Only Title Only Author and Title

Mejias, J., Truong, N.M., Abad, P., Favery, B., and Quentin, M. (2019) Plant proteins and processes targeted by parasitic nematode effectors. Frontiers in Plant Science, 10, 970.
Google Scholar: Author Only Title Only Author and Title

Mitchum, M.G., Hussey, R.S., Baum, T.J., Wang, X., Elling, A.A., Wubben, M., and Davis, E.L. (2013) Nematode effector proteins: an emerging paradigm of parasitism. New Phytologist, 199, 879–894.
Google Scholar: Author Only Title Only Author and Title

Mitchum, M.G., Wang, X., Wang, J., and Davis, E.L. (2012) Role of nematode peptides and other small molecules in plant parasitism. Annual Review of Phytopathology, 50, 175–195.
Google Scholar: Author Only Title Only Author and Title

Muhire, B.M., Varsani, A., and Martin, D.P. (2014) SDT: a virus classification tool based on pairwise sequence alignment and identity calculation. PLoS ONE, 9, e108277.
Google Scholar: Author Only Title Only Author and Title

Nguyen, C.-N., Perfus-Barbeoch, L., Quentin, M., Zhao, J., Magliano, M., Marteu, N., et al. (2018) A root-knot nematode small glycine and cysteine-rich secreted effector, MiSGCR1, is involved in plant parasitism. New Phytologist, 217, 687–699.
Google Scholar: Author Only Title Only Author and Title

O'Connell, R.J. and Panstruga, R. (2006) Tete a tete inside a plant cell: establishing compatibility between plants and biotrophic fungi and oomycetes. New Phytologist, 171, 699–718.
Google Scholar: Author Only Title Only Author and Title

Olmo, R., Cabrera, J., Díaz-Manzano, F.E., Ruiz-Ferrer, V., Barcala, M., Ishida, T., et al. (2020) Root-knot nematodes induce gall formation by recruiting developmental pathways of post-embryonic organogenesis and regeneration to promote transient pluripotency. New Phytologist, 227, 200–215.
Google Scholar: Author Only Title Only Author and Title

Opperman, C.H., Bird, D.M., Williamson, V.M., Rokhsar, D.S., Burke, M., Cohn, J., et al. (2008) Sequence and genetic map of Meloidogyne hapla: A compact nematode genome for plant parasitism. Proc Natl Acad Sci U S A, 105, 14802–14807.
Google Scholar: Author Only Title Only Author and Title

Peeters, N., Carrère, S., Anisimova, M., Plener, L., Cazalé, A.-C., and Genin, S. (2013) Repertoire, unified nomenclature and evolution of the Type III effector gene set in the Ralstonia solanacearum species complex. BMC Genomics, 14, 859.
Google Scholar: Author Only Title Only Author and Title

Quentin, M., Abad, P., and Favery, B. (2013) Plant parasitic nematode effectors target host defense and nuclear functions to establish feeding cells. Frontiers in Plant Science, 4, 53.
Google Scholar: Author Only Title Only Author and Title

Rancurel, C., van Tran, T., Elie, C., and Hilliou, F. (2019) SATQPCR: website for statistical analysis of real-time quantitative PCR data. Molecular and Cellular Probes, 46, 101418.
Google Scholar: Author Only Title Only Author and Title

Reddy, A.S.N., Marquez, Y., Kalyna, M., and Barta, A. (2013). Complexity of the alternative splicing landscape in plants. The Plant Cell, 25, 3657–3683.
Google Scholar: Author Only Title Only Author and Title

Rigo, R., Bazin, J., Crespi, M., and Charon, C. (2019). Alternative splicing in the regulation of plant-microbe interactions. Plant and Cell Physiology, 60, 1906–1916.
Google Scholar: Author Only Title Only Author and Title

Rodiuc, N., Vieira, P., Banora, M.Y., and de Almeida Engler, J. (2014) On the track of transfer cell formation by specialized plant-parasitic nematodes. Frontiers in Plant Science, 5, 1–14.
Google Scholar: Author Only Title Only Author and Title

Roux, B., Bolot, S., Guy, E., Denancé, N., Lautier, M., Jardinaud, M.-F., et al. (2015) Genomics and transcriptomics of Xanthomonas campestris species challenge the concept of core type III effectome. BMC Genomics, 16, 975.
Google Scholar: Author Only Title Only Author and Title

Rutter, W.B., Hewezi, T., Abubucker, S., Maier, T.R., Huang, G., Mitreva, M., et al. (2014) Mining novel effector proteins from the esophageal gland cells of Meloidogyne incognita. Molecular plant-microbe interactions, 27, 965–974.
Google Scholar: Author Only Title Only Author and Title

van Schie, C.C.N. and Takken, F.L.W. (2014) Susceptibility genes 101: how to be a good host. Annual Review of Phytopathology, 52, 551–581.
Google Scholar: Author Only Title Only Author and Title

Schmitt-Keichinger, C. (2019) Manipulating cellular factors to combat viruses: a case study from the plant eukaryotic translation initiation factors eIF4. Frontiers in Microbiology, 10:17. doi: 10.3389/fmicb.2019.00017
Google Scholar: Author Only Title Only Author and Title

Singh, S.K., Hodda, M., and Ash, G.J. (2013) Plant-parasitic nematodes of potential phytosanitary importance, their main hosts and reported yield losses. EPPO Bulletin, 43, 334–374.
Google Scholar: Author Only Title Only Author and Title

Somvanshi, V.S., Tathode, M., Shukla, R.N., and Rao, U. (2018) Nematode genome announcement: a draft genome for rice root-knot nematode, Meloidogyne graminicola. Journal of Nematology, 50, 111–116.
Google Scholar: Author Only Title Only Author and Title

Staiger, D. and Brown, J.W.S. (2013). Alternative splicing at the intersection of biological timing, development, and stress responses. Plant Cell, 25, 3640–3656.
Google Scholar: Author Only Title Only Author and Title

Susič, N., Koutsovoulos, G.D., Riccio, C., Danchin, E.G.J., Blaxter, M.L., Lunt, D.H., et al. (2020) Genome sequence of the root-knot nematode Meloidogyne luci. Journal of Nematology, 52, e2020-25.
Google Scholar: Author Only Title Only Author and Title

Tan, G., Liu, K., Kang, J., Xu, K., Zhang, Y., Hu, L., Zhang, J. and Li, C. (2015) Transcriptome analysis of the compatible interaction of tomato with Verticillium dahliae using RNA-sequencing. Frontiers in Plant Science, 6, 428.
Google Scholar: Author Only Title Only Author and Title

Tomalova, I., Iachia, C., Mulet, K., and Castagnone-Sereno, P. (2012) The map-1 gene family in root-knot nematodes, Meloidogyne spp.: a set of taxonomically restricted genes specific to clonal species. PloS one, 7, e38656.
Google Scholar: Author Only Title Only Author and Title

Toruño, T.Y., Stergiopoulos, I., and Coaker, G. (2016) Plant-pathogen effectors: cellular probes interfering with plant defenses in spatial and temporal manners. Annual Review of Phytopathology, 54, 419–441.
Google Scholar: Author Only Title Only Author and Title

Truong, N.M., Nguyen, C.-N., Abad, P., Quentin, M., and Favery, B. (2015) Function of root-knot nematode effectors and their targets in plant parasitism. Advances in Botanical Research, 73, 293–324.
Google Scholar: Author Only Title Only Author and Title

Velasquez, A., Chakravarthy, S., and Martin, G.B. (2009) Virus-induced gene silencing (VIGS) in Nicotiana benthamiana and tomato. Journal of Visualized Experiments, 28, 1292. doi: 10.3791/1292.

Google Scholar: Author Only Title Only Author and Title

Verma, A. et al. (2018). The novel cyst nematode effector protein 30D08 targets host nuclear functions to alter gene expression in feeding sites. New Phytologist, 219, 697–713.
Google Scholar: Author Only Title Only Author and Title

Wang, X., Xue, B., Dai, J., Qin, X., Liu, L., Chi, Y., et al. (2018) A novel Meloidogyne incognita chorismate mutase effector suppresses plant immunity by manipulating the salicylic acid pathway and functions mainly during the early stages of nematode parasitism. Plant Pathology, 67, 1436–1448.
Google Scholar: Author Only Title Only Author and Title

Yamaguchi, Y.L., Suzuki, R., Cabrera, J., Nakagami, S., Sagara, T., Ejima, C., et al. (2017) Root-knot and cyst nematodes activate procambium-associated genes in Arabidopsis roots. Frontiers in Plant Science, 8, 1195. doi: 10.3389/fpls.2017.01195
Google Scholar: Author Only Title Only Author and Title

Yang, Y., Jittayasothorn, Y., Chronis, D., Wang, X., Cousins, P., and Zhong, G.-Y. (2013) Molecular characteristics and efficacy of 16D10 siRNAs in inhibiting root-knot nematode infection in transgenic grape hairy roots. PloS one, 8, e69463.
Google Scholar: Author Only Title Only Author and Title

Zheng, Y. Ding, B., Fei, Z. and Wang, Y. (2017a) Comprehensive transcriptome analyses reveal tomato plant responses to tobacco rattle virus-based gene silencing vectors. Scientific Reports, 7, 9771
Google Scholar: Author Only Title Only Author and Title

Zheng, Y., Wang, Y., Ding, B., Fei, Z., and Simon, A.E. (2017b). Comprehensive transcriptome analyses reveal that Potato Spindle Tuber Viroid triggers genome-wide changes in alternative splicing, inducible trans-acting activity of phased secondary small interfering RNAs, and immune responses. Journal of Virology, 91, 247–264.
Google Scholar: Author Only Title Only Author and Title

Zhu, C., Li, X. and Zheng, J. (2018) Transcriptome profiling using Illumina- and SMRT-based RNA-seq of hot pepper for in-depth understanding of genes involved in CMV infection. Gene, 666, 123-133.
Google Scholar: Author Only Title Only Author and Title